bulk solids handling Volume 2, Number 2, June 1982

Reclaim Power and Geometry of Bin Interfaces in Belt and Apron Feeders

An Analytical Approach

F.J.C. Rademacher, The Netherlands

Summary

Based on common sense measures and a simplified physical model, some design criteria are given for achieving proper dimensioning of bin interfaces in the case of belt and apron feeders. How the reclaim power, closely related to wear, depends on the geometry of the interface between silo and feeder is discussed. The characteristics of both declined and inclined feeders are included in the analysis. From this it is estimated to what extent the performance of inclined feeders differs from that of horizontal ones.

List of Symbols*

a	Aperture	m
d	Height of dams on feeder pans	m
E_s	Specific reclaim energy	1
E_{s_w}	Specific reclaim energy in case of inferior design	1
F	Friction force at feeder plates	N
F_b	Interbulk force at feeder plates	N
F_{b_h}	Horizontal component of F_b	N
F_{b_v}	Vertical component of F_b	N
F_s	Friction force on both side skirts	N
F_s'	Friction force on both side skirts in the case of the inferior design	N
F_s''	Equivalent skirt friction force caused by the aperture rim in inferior design	N
F_{s_w}	Total skirt friction force in inferior design ($= F_s' + F_s''$)	N
g	Gravity	m/sec²
h	Average height of the interfacial bed of material	m
h_e	Effective height of the side skirts	m
h_e''	Effective height of that part of the side skirts not being covered with "dead comer" material	m
H_f	Surcharge during flow, expressed in material head	m
H_i	Initial surcharge expressed in material head	m
k	Rankine's ratio	1
l	Length of slotted hopper outlet	m
l'	Length over which the side skirts are covered with "dead corner" material	m
l''	Length over which the side skirts are not covered with "dead corner" material	m
l_{s_1}	Width of the plate dams	m
l_{s_2}	Length of the plate section over which the bulk material will slide in case slip might occur (dam provided plate)	m
l_r	Length of the dead corner section of a dam provided plate	m
N	Normal force on plate	N
p	Pitch of feeder plates	m
P	Required net feeder power	Nm/sec
Q	Volumetric reclaim rate	m³/sec
r	Rim-width at aperture	m
R_1	Resultant force exerted on the interfacial material bed by the feeder during flow	N
R_2	Resultant force exerted on top of the interfacial material bed by the surcharge of the material in the silo during flow	N
ReP	Reclaim power	Nm/sec
t	Time	sec
T	Required belt traction of feeder	N
T_w	Required belt traction of feeder in inferior design	N
v_B	Average bulk velocity through aperture	m/sec
v_b	Velocity of feeder belt	m/sec
w	Average width of the slotted hopper outlet	m
W	Weight of the interfacial material bed	N
X	Auxiliary quantity	1
Y	Auxiliary quantity	1
α	Half the hopper wedge angle	rad.

* Some of the quantities listed here were non-dimensionalised in the text by adding the symbol o.

Prof. Dr. Ir. F J. C. Rademacher, University of Twente, P.O. Box 217, Enschede Drienerlo, The Netherlands

β	Angle of release at which the schematized shearing zone, being the top of the interfacial material bed, is supposed to settle	rad.
γ	Specific weight	N/m³
δ	Clearance between skirt and feeder at the upstream end	m
ϵ	Skirt height coefficient, accounting for the small releasing clearance between side skirts and feeder	1
θ	Feeder inclination	rad.
μ_b	Friction coefficient at ordinary flat plate feeder belt	1
μ_{b_d}	Apparent coefficient of friction at feeder, obtainable by providing a flat plated feeder belt with dams	1
μ_{i_f}	Internal coefficient of friction of bulk material during flow	1
μ_{i_i}	Internal coefficient of friction of bulk material during initial, or "break-away", condition	1
ξ	Average bulk velocity at aperture relative to feeder belt speed	1
ϱ	Bulk density	kg/m³
σ	Average vertical normal stress at interface of bulk material and feeder during flow	N/m²
σ_1	Average normal stress at interface of bulk and aperture rim during flow, for inferior design	N/m²
σ_2	Average normal stress at interface of "dead corner" bulk and side skirt for flow condition for inferior design	N/m²
σ_{a_h}	Average horizontal stress in the interfacial material bed for flow condition	N/m²
σ_{a_v}	Average vertical stress in the interfacial material bed during flow	N/m²
τ	Fully mobilised shear stress at interface of bulk material and feeder plates	N/m²
ϕ_b	Friction angle at ordinary flat plate feeder belt	rad.
ϕ_{b_e}	Effective or mobilized friction angle at ordinary flat plate feeder belt	rad.
ϕ_{i_a}	Apparent angle of friction at the shearing zone, schematically represented by the top plane of the interfacial material bed during flow	rad.
ϕ_{i_f}	Angle of internal friction during flow	rad.
ϕ_{i_i}	Angle of internal friction at initial, or "break-away", condition	rad.
ϕ_w	Angle of friction at the hopper wall	rad.
χ	Angle between major principal stress and normal to hopper wall for flow conditions	rad.
ψ	Force coefficient defined by Eq. (19)	1
ψ_w	Force coefficient for inferior design defined by Eq. (29)	1

1. Introduction

In an earlier publication [5] an approximate analysis was developed for the dimensioning of bin openings having horizontally positioned belt or apron feeders underneath. Even so, the author has still seen feeders malfunctioning for several reasons. Therefore, in what follows, more attention will be paid to these feeders, including flow promotion measures, to the dimensioning of the bin aperture and to the estimation of the required reclaim power.

1.1 Design Details

Fig. 1 shows one of the most simple designs. The aperture a arises from cutting off the bin bottom at an angle of release β to the feeder. A basic drawback is that the angle of release in the horizontal plane can become unnecessarily large, depending on the wedge angle of the hopper and the ratio between width w, length l and aperlure a. Without side skirts the required width of the apron feeder amounts to at least double the upstream width w of the bin outlet even in the case where the aperture is as small as $0.3\,w$. For $a = w$, the feeder width has to be $4\,w$. By means of side skirts, not shown in Fig. 1, the width necessary can easily be restricted for the examples mentioned, to $1.5\,w$ and $2\,w$, respectively, which is still large compared to more sophisticated solutions that will be discussed later. The angle of release in plan, being dependent on the aperture a, remains the most significant disadvantage of the simple design of Fig. 1.

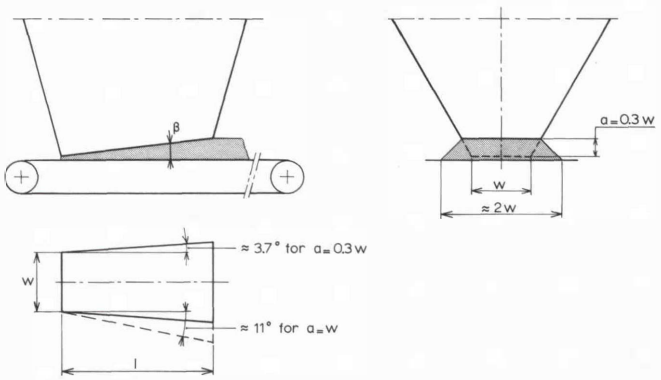

Fig. 1: Illustrating that for the most simple design a relatively small aperture of $0.3\,w$ can lead in plan to a semi release angle of 3.7°, while for $a = w$ this angle can be as large as 11°

Fig. 2 shows an "improved" design in the sense that the downstream end of the hopper outlet has been provided with an adjustable aperture be means of a gate and sliding valve. The corresponding angle of release β occurs within the hopper side walls. The lower rims of the latter enclose a small release angle to the feeder in order to prevent jamming of lumps. Regrettably, this version is often installed in spite of also being an inferior design type. The apparent constructional and economical advantages of having an adjustable aperture with no side skirts at all, are counteracted by the dead corners just before the aperture, as shown in Sections n-n and m-m of Fig. 2. The bulk material tends to stick in these corners causing local stream convergence between rough walls.

In the design of Fig. 3 the drawbacks of the preceding two designs have been avoided. The two vertical side skirts, of

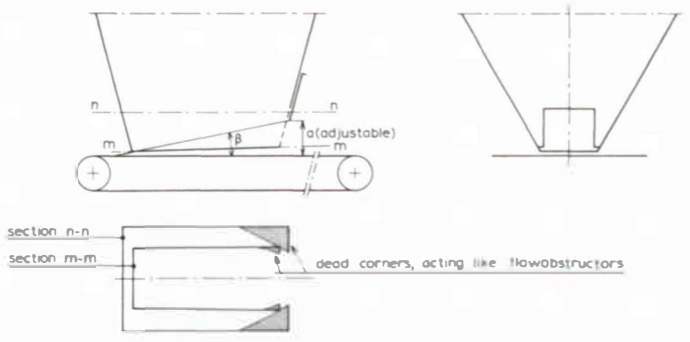

Fig. 2: By means of gate and sliding plate valve the aperture a is adjustable independently of the angle of release in plan. However, dead corners just before the gate cause flow obstructions (Section m-m and n-n)

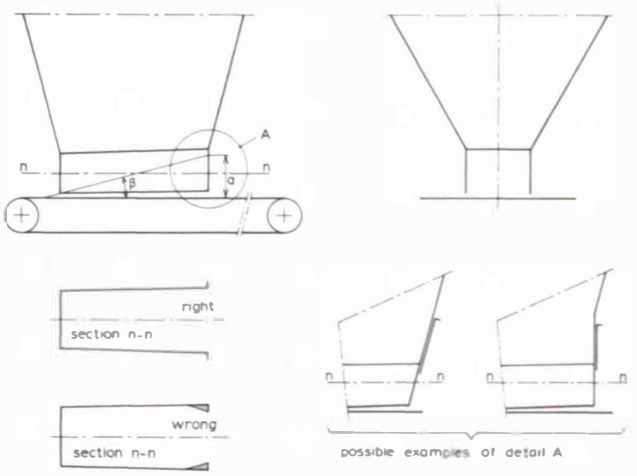

Fig. 3: Application of relatively high side skirts, a slide adjusted aperture and a well designed surrounding (A) of the aperture can lead to a continuously diverging flow with no obstructions at all

considerable height, enclose an angle of release in plan. They also maintain a release angle to the feeder for the reasons already mentioned.

Just as in the preceding cases, the actual aperture at A is achieved by adjusting a sliding plate valve. The lower right hand comer of the figure shows two well designed apertures. However, the flanges where the valve-guides are attached should be positioned outward of the side skirts in order not to obstruct the flow, as shown in the lower left hand comer of Fig. 3.

The possible consequences of ignoring these small but important design rules are discussed in the next section.

2. Proper Dimensioning of the Bin Aperture; Power Requirements

2.1 Geometry

The required bin-aperture a, Fig. 3, follows from the quasi-static equilibrium of the bed of material enclosed in the transition zone ABCDEFGH, Fig. 4. In calculating this, use will be made of the simplified model that has been discussed earlier [5]. The assumptions on which this model is based are therefore briefly repeated:

1. Top plane

The resultant force R_2 exerted on the assumed plane of rupture EFGH encloses the apparent internal angle of friction ϕ_{i_a} with the normal n. The vertical pressure on this plane can be estimated by the use of existing theories [2, 7, 8, 12, 19], and so follows the magnitude of the resulting force R_2. More attention to this overpressure is paid in Appendix 1 and in the example to be discussed later.

2. Lower plane

The resulting force R_1 on plane ABCD encloses an effective angle of friction ϕ_{b_e} with the normal, smaller than the friction angle ϕ_b at the interface of feeder and bulk material.

3. Weight of the bed material

The weight of the material in the transition zone cannot be neglected and will therefore be considered in the calculations.

4. Rear plane

The resulting force on plane ADEH is evidently zero.

5. Cross-section at aperture

The resulting force on cross-section BCFG can be neglected.

6. Side skirts

The frictional forces exerted by the side skirts on planes ABEF and CDGH (F_s in total) are negligible in most cases. They will nevertheless be considered in the calculations as they can limit the maximal obtainable inclination ϕ.

It thus follows that the equilibrium of the material entrapped in the transition zone is basically governed by the resulting forces on the top and bottom planes R_2 and R_1, the weight of the bed material W, and to a minor extent, by the friction F_s on the side skirts. These forces are shown in Fig. 4. From the vertical and horizontal equilibrium follows:

$$F_s \sin\theta + W + R_2 \cos(\phi_{i_a} - \beta - \theta) = R_1 \cos(\phi_{b_e} - \theta) \quad (1)$$

$$F_s \cos\theta + R_2 \sin(\phi_{i_a} - \beta - \theta) = R_1 \sin(\phi_{b_e} - \theta) \quad (2)$$

where:

$$W \simeq h w l \varrho g \quad (3)$$

The latter approximation holds within 8% even for a total release angle between the skirts as large as 10° and an aperture of 0.9, δ being 0.1. The vertical pressure on the top plane EFGH can be calculated with the present theory summarised in Appendix 1. Other theories may lead to considerable differences. Whatever the different results may be, the vertical pressure can always be expressed as an equivalent head of material H_f, which is used in the following equilibrium equations:

$$R_2 \cos(\phi_{i_a} - \beta - \theta) \simeq H_f \cdot \varrho g \cdot w l \cos(\phi + \beta) \quad (4)$$

$$R_2 \sin(\phi_{i_a} - \beta - \theta) \simeq H_f \cdot \varrho g \cdot w l \cos(\phi + \beta) \tan(\phi_{i_a} - \beta - \theta) \quad (5)$$

From Appendix 2 it follows that for the friction forces F_s exerted by the side skirts:

$$F_s \simeq \frac{3}{2} k \mu_s \left(H_f + \frac{h_e}{2 \cos\theta} \right) \varrho g h_e l \quad (6)$$

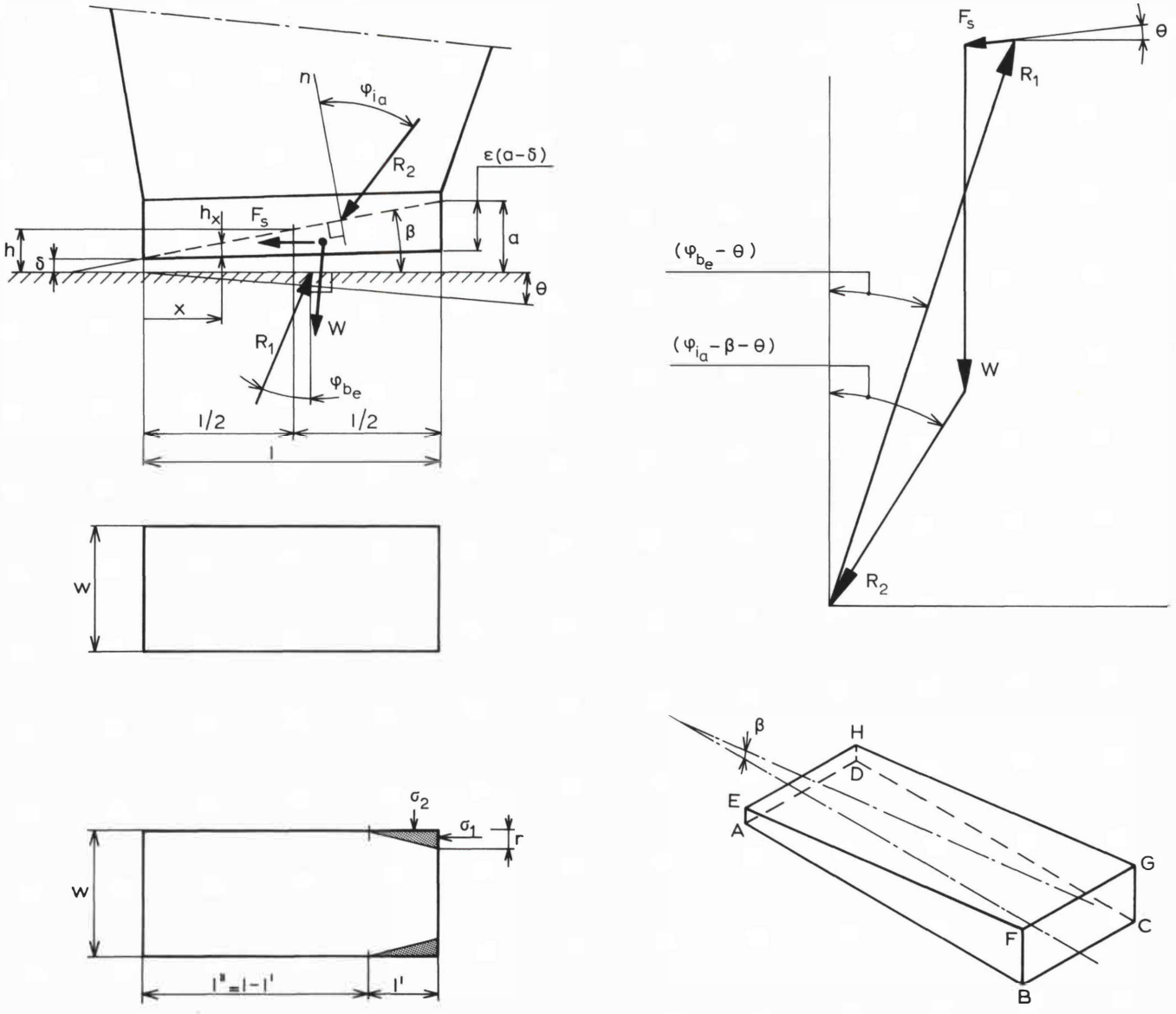

Fig. 4: The equilibrium of the interfacial zone of bulk solid

in which

$$h_e = \frac{2}{3}\,\epsilon\,(a - \delta) \tag{7}$$

h_e = the effective height of the side skirt

k = the ratio between the minor and major principal stress in a plane inside the bed material, parallel to ABCD, $(0 < k < 1)$

ϵ = coefficient, accounting for the clearance between the lower rim of the side skirts and the feeder

μ_s = coefficient of kinetic friction at the interface of the bulk and side skirts.

For practical reasons all dimensions, including the static head H_f, will be related to the average width w leading to the following dimensionless quantities:

$$a_o = a/w \tag{8}$$

$$\delta_o = \delta/w \tag{9}$$

$$h_o = h/w, \text{ resp. } h_{e_o} = h_e/w \tag{10}$$

$$H_{f_o} = H_f/w \tag{11}$$

$$l_o = l/w \tag{12}$$

Substitution of (3) to (6) in the quotient of (2) and (1), and incorporating (8) to (12) leads to:

$$\tan(\phi_{b_e} - \theta) \simeq \frac{H_{f_o}\cos(\theta + \beta)\cdot\tan(\phi_{i_a} - \beta - \theta) + \frac{3}{2}\,k\mu_s\left(H_{f_o} + \frac{h_{e_o}}{2\cos\theta}\right)h_{e_o}\cos\theta}{H_{f_o}\cos(\theta + \beta) + h_o + \frac{3}{2}\,k\mu_s\left(H_{f_o} + \frac{h_{e_o}}{2\cos\theta}\right)h_{e_o}\sin\theta} \tag{13}$$

in which

$$h_o = 0.5(\delta_o + a_o), \quad h_{eo} = \frac{2}{3}\epsilon(\alpha_o - \delta_o) \tag{14}$$

and

$$\beta = \arctan\frac{a_o - \delta_o}{l_o} \tag{15}$$

For a given geometry, inclusive of the static head, i.e., when δ_o; a_o; l_o; H_o; θ; ϕ_{ia}; ϵ and μ_s are known, in using (14) and (15) the right hand member of (13) can be calculated supposing that

$$k = (1 - \sin\phi_{ia})/(1 + \sin\phi_{ia})$$

The required effective angle of friction at the feeder (ϕ_{be}) then follows simply from the left hand side, as does μ_{be}.

2.2 The Required Belt Pull and Reclaim Power

The required steady-state feeder power P equals the product of belt traction T and belt velocity v_b. The belt traction equals:

$$T = R_1 \cdot \sin\phi_{be} \tag{17}$$

Substitution of (5) and (6) in (2), and incorporating (8) to (12) leads to:

$$R_1 = \psi \cdot H_f \cdot \varrho g \cdot wl \tag{18}$$

in which

$$\psi = \frac{\frac{3}{2}k\mu_s\left(1 + \frac{1}{2\cos\theta}\frac{h_{eo}}{H_{fo}}\right)h_{eo}\cdot\cos\theta + \tan(\phi_{ia} - \beta - \theta)\cdot\cos(\theta + \beta)}{\sin(\phi_{be} - \theta)} \tag{19}$$

Substitution of (18) in (17) and incorporating (11) and (12) results in:

$$T = \psi \cdot \sin\phi_{be} \cdot H_{fo} \cdot l_o \cdot w^3 \varrho g \tag{20}$$

or in dimensionless form:

$$T_o = \left(\frac{T}{w^3 \varrho g}\right) = \psi \cdot \sin\psi_{be} \cdot H_{fo} \cdot l_o \tag{21}$$

giving a dimensionless number for the belt pull.

The required steady state feeder power equals:

$$P = R_1 \cdot \sin\phi_{be} \cdot v_b = \psi \cdot \sin\phi_{be} \cdot H_{fo} \cdot l_o w^3 \varrho g \cdot v_b \tag{22}$$

or in dimensionless form:

$$P_o = \left(\frac{P}{w^3 \varrho p\, v_b}\right) = \psi \sin\phi_{be} \cdot H_{fo} \cdot l_o \tag{23}$$

Of more interest than the required feeder power may be the work used per unit volume of reclaimed bulk material. However, for the purpose of this paper preference will be given to a dimensionless expression, referred to in the following as specific energy E_s, being the quotient of the work for each unit volume of reclaimed bulk material and the Reclaim Performance ReP. The latter is defined as the product of the specific weight of the bulk material and the average horizontal displacement of the material along the bin opening [1]. In reality, the actual reclaim performance will increase with both the overpressure on the material in the interfacial zone and its horizontal displacement. Elevating the material is not a primary task of feeders and is therefore eliminated in the definition of reclaim performance. The reclaim performance in Δt seconds amounts to:

$$ReP = (Q\,\Delta t)(\varrho g)\left(\frac{l\cos\theta}{2}\right) \tag{24}$$

in which

$$Q = v_B \cdot a \cdot w \tag{25}$$

v_B being the average velocity of the bulk across the aperture for which the following holds:

$$v_B = \xi \cdot v_b, \quad (0 < \xi \leqq 1) \tag{26}$$

So it follows that:

$$ReP = \frac{1}{2}\xi \cdot \cos\theta \cdot \varrho g \cdot awl \cdot v_b \cdot \Delta t$$

or:

$$ReP = \frac{1}{2}\xi \cdot \cos\theta \cdot a_o \cdot l_o \cdot w^3 \varrho g \cdot v_b \cdot \Delta t \tag{27}$$

The energy supplied follows from (22). The specific energy then appears as:

$$E_s = \left(\frac{P \cdot \Delta t}{ReP \cdot \Delta t}\right) = \frac{2\psi \sin\phi_{be}}{\xi\cos\theta}\left(\frac{H_{fo}}{a_o}\right) \tag{28}$$

Summarising, the dimensionless number for the required feeder power P_o, being equal to that for the belt pull T_o, amounts to $\psi \cdot \sin\phi_{be} \cdot H_{fo} \cdot l_o$, while the specific energy follows from (28).

2.3 Graphical Representation

1. Horizontal arrangement

Fig. 5 shows some cases for horizontal feeders. It is evident that a large aperture reduces the effective coefficient of friction at the feeder μ_{be} considerably. This is also favoured, although to a lesser extent, by a smaller relative length l_o of the slotted hopper outlet (Figs. 5a and b). As can be seen from Figs. 5c and d, μ_{be} increases with increasing head load and inevitably almost linearly with the apparent internal coefficient of friction of the bulk material μ_{ia}. Figs. 5e and f show some examples for the required specific energy E_s and belt pull T_o. The specific energy increases excessively with decreasing aperture, showing that large energy savings, per reclaimed quantity of bulk material, of 80 % and more can be achieved at large apertures. This is a clear indication that the aperture should be made as large as possible in compliance with hopper geometry, bulk properties and head load and that the throughput must principally be controlled by the feeder speed and *not* by valve adjustment.

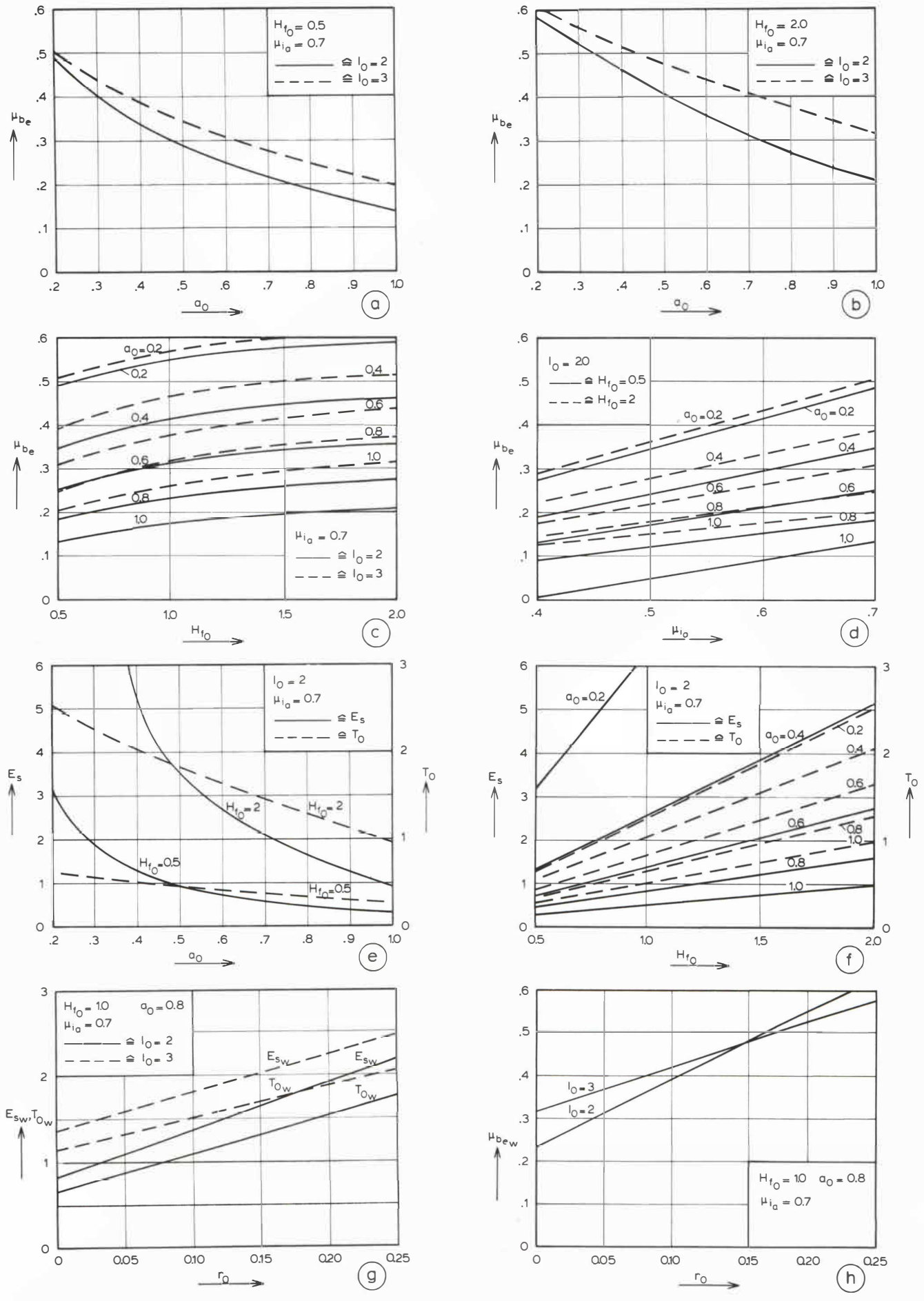

Fig. 5: Horizontal apron feeder, $\theta = 0$; $\epsilon = 0.9$; $\xi = 1$; $\delta_0 = 0.1$

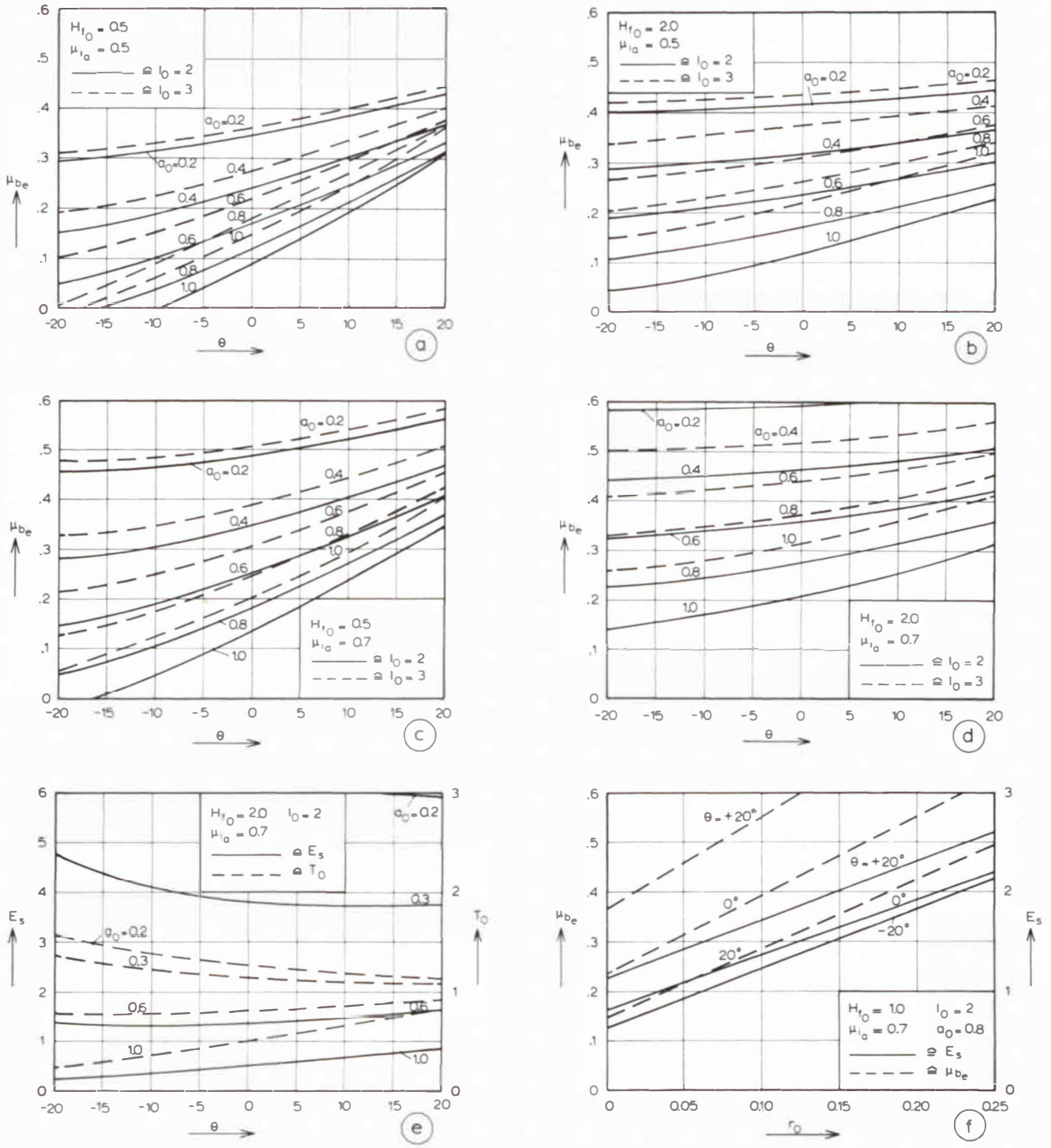

Fig. 6: Inclined apron feeder, $-20° \leq \theta \leq 20°$. $\epsilon = 0.9$; $\xi = 1$; $\delta_0 = 0.1$

2. Inclined arrangement

Wall friction coefficients between bulk materials and flat steel walls mostly do not exceed 0.4. Figs. 6a to 6d clearly show that the inclination of feeders, whenever possible, is rather limited and preferably should be avoided completely. Where a safety factor of 1.5 against slip is considered reasonable, the allowable effective coefficient of friction at the belt amounts to 0.4/1.5 ≃ 0.27. The allowable inclination in the cases of Figs. 6a, c and d is then limited to 16.7°, 13°, and 13°, respectively, with an aperture of unity and relative slot length of 2. Only the less realistic case of high overpressure (H_{f_0} = 2) and low internal friction (μ_{i_a} = 0.5), Fig. 6b, allows for considerably larger angles of inclination. The inevitable conclusion arises that for a realistic material ($\mu_{i_a} \simeq 0.7$), possible inclination angles will increase with increasing apertures and large specific overpressures H_{f_0}. Apart from the question as to what extent the latter can be changed, it is interesting to note from Fig. 6e that, although the required traction and specific energy at large apertures do decrease with increasing declination, the opposite holds

for small apertures. The explanation lies basically in the assumed constant vertical pressure on the plane of rupture which will be considered in the following with reference to Fig. 4. If, by way of example, the inclination is reduced from $+20°$ to $-20°$ the clockwise rotation of R_2 amounts to 40° while its vertical component does not change very much. Simultaneously R_1 has been increased considerably and rotated clockwise also, but over a somewhat smaller angle, leading to a smaller μ_{be}. The increase in R_1 can overtake the decrease of sin ϕ_{be} in which case, according to (17), a larger traction will be required.

2.4 Conclusion

If an inclined arrangement cannot be avoided, depending on the results of the curves given, it may be advisable to provide the feeder plates with ribs to increase the apparent coefficient of friction. The effect obtainable is discussed further in Appendix 4.

3. Wrong Dimensioning of the Bin Aperture; Power Requirements

3.1 Geometry

In the case of the inferior design illustrated in the lower left corner of Figs. 3 and 4, the flow obstruction in the form of the fixed bulk in the corners just before the aperture can be considered to be equivalent to an extra skirt friction as calculated in Appendix 3. Equation (13) then becomes:

$$\tan(\phi_{b_{ew}} - \theta) \simeq \frac{H_{f_o} \cos(\theta + \beta) \cdot \tan(\phi_{i_a} - \beta - \theta) + \left(\frac{F_{swo}}{l_o}\right) \cos\theta}{H_{f_o} \cos(\theta + \beta) + h_o + \left(\frac{F_{swo}}{l_o}\right) \sin\theta} \qquad (16)$$

where F_{swo} stands for the efficient, dimensionless, skirt friction as mentioned by way of example in Appendix 3. Angle $\phi_{b_{ew}}$ stands for the required effective angle of friction for the case of this inferior design.

3.2 The Required Belt Pull and Reclaim Power

In the case of the inferior design of Fig. 3, the expression for ψ (19) changes to:

$$\psi_w = \frac{\left(\frac{F_{swo}}{H_{f_o} l_o}\right) \cos\theta + \cos(\theta + \beta) \cdot \tan(\phi_{i_a} - \beta - \theta)}{\sin(\phi_{b_{ew}} - \theta)} \qquad (29)$$

and must be used instead of ψ in equations (20) to (23), and (28). F_{swo} is elaborated in Appendix 3.

3.3 Graphical Representation

1. Horizontal arrangement

The disastrous effect of an inwardly directed guide-way for the valve can be estimated from the examples in Figs. 5g and h. For a rim-width r_o of 10 %, for instance, the increase of required traction and specific energy amounts to $\simeq$ 67 % and 33 % for l_o = 2 and 3, respectively. At the same time the required effective coefficient of friction at the feeder μ_{be} increases also by $\simeq$ 67 % and 33 %.

2. Inclined arrangement

For the example in Fig. 6f it holds that a 10 % guide-rim r_o causes an increase of 41 % in the required specific energy within an inclination range of $-20°$ to $+20°$. The majority of this increase lies within the range $0 < \theta \leqq 20°$. However, it is very clear from Fig. 6f that the required effective coefficient of friction at the feeder μ_{be} can rise very quickly above realistic values with increasing r_o.

4. Feeder Loads and Required Drive

Feeder loads do not vary only with differences in bin design and the bulk materials to be handled. Even for one particular combination of bin and bulk material great differences in feeder load can occur, as the initial load during, or just after, filling is normally far in excess of the load during emptying under steady flow. A factor of 5 is not exceptional. Of the existing theoretical and empirical approximations [2, 7, 8, 12, 19] those of Jenike [19] and Arnold, McLean and Roberts [2] will be cited and used in an example as they cover the Hager experiments most successfully with an accuracy of approximately 25 % for steady flow conditions [17, 18].

Their solution for a chisel type hopper with a slotted opening is quoted in Appendix 1. The existing theoretical estimates for the initial feeder loads are not very useful as they are based on assumed physical phenomena that are not likely to occur in practice. However, from the careful, large scale, experiments of Hager, it follows that the anticipation of break-away loads of about 5 times the load during steady flow conditions will suffice for design purposes of apron feeders. On the one hand allowable start-torque overload of electric motors amounts to 60—100 % for a period of 15 to 20 seconds, on the other, the break-away torque for most feeders is reduced to the level for steady flow conditions within a travel distance on the feeder belt of two to three times the average size of the upper 5 % sized bulk particles. This means that in the great majority of cases the break-away torque will last no longer than a small fraction of the allowable overload time of the electric motor. It is on this basis and the selected kind of speed reduction between motor and feeder shaft that the motor size should be dimensioned. In so doing the designer should clearly bear in mind the valuable design rules given by Jenike [19] in order to keep the feeder load as small as possible. Too many oversize motors still do occur in practice partly because of overestimation of the break-away torque and partly because of too small a range of adjustable speed reduction. This latter results in operation at very low capacities only being possible by adjustment of the valve (aperture reduction), increasing the required torque excessively. Ideal for apron feeders is therefore a drive unit that can generate a high

break-away torque for just a few seconds and that has a range of continuously variable speeds covering all the required flow capacities at the maximum possible gate opening for the bulk material to be handled. Second best is a limited number of adjustable speeds. The required throughput is then obtained by starting at the maximum allowable gate opening and in selecting the lowest speed that results in a capacity just a little too large. Although further adjustment has to be achieved by lowering the valve the latter is at least limited and so is the waste of reclaim energy. The larger the adjustable number of speeds, the smaller this energy waste will be.

5. Experiments

Experiments have been carried out with a perspex hopper model, provided with an electrically driven horizontal belt conveyor suspended by three vertical steel wires each of which is attached to the feeder frame via a dynamometer, Fig. 8. These three dynamometers serve to measure the vertical feeder load. A fourth dynamometer, horizontally arranged, serves to measure the friction force exerted by the belt on the bulk solid. All four forces are continuously recorded. The bulk flow at the hopper walls and the side skirts was filmed for a part of the experiments. The characteristics of the device are shown in Figs. 7 and 8.

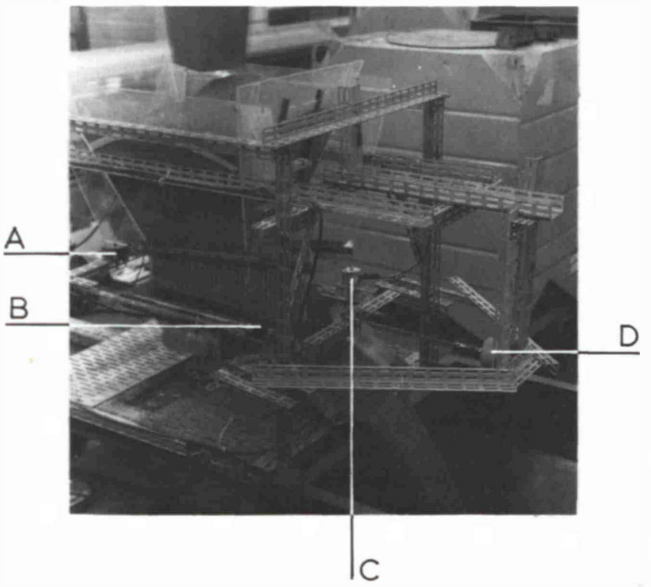

Fig. 8: View of the test apparatus

Tests were carried out with cylindrical plastic granules of 2.7 mm diameter, varying in length from 5 to 8 mm, spinach speed, potato starch and Russian peas. Steady state belt speed varied from 9 to 21 cm/sec; apertures up to 10 cm. An extra container with feeder, full of bulk solid, was situated above the device in order to keep the hopper filled to a fixed level. After filling, the belt was started at a pre-set velocity enabling the recording of the break-away force. Tests were performed for a series of pre-set, increasing, apertures. The

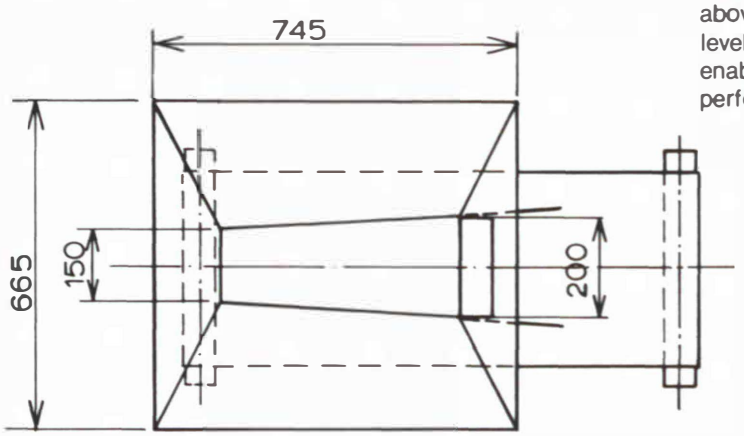

Fig. 7: Dimensions of the test device

dimensions in mm

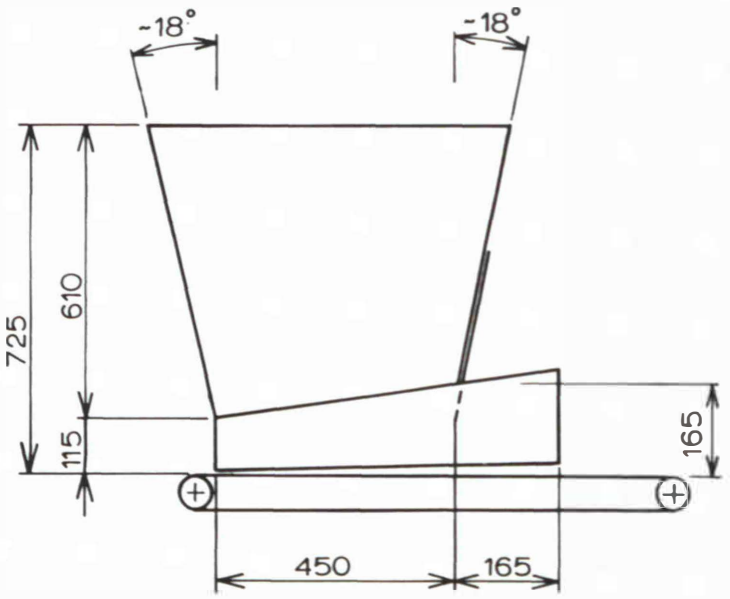

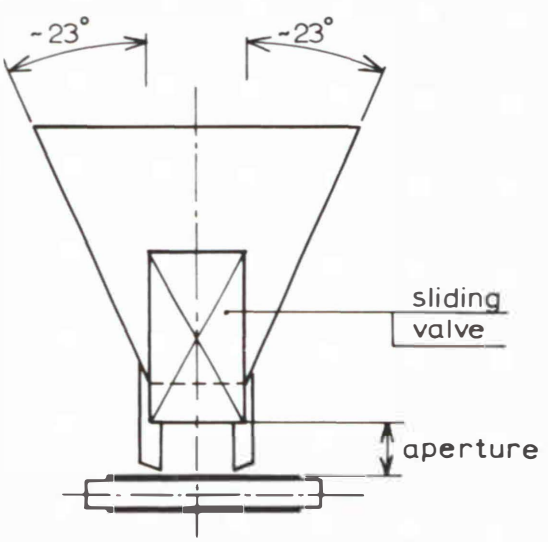

inclination being zero, it follows from Equations (1) and (2) that:

$$\mu_{ia} = \tan\left\{\beta + \arctan\frac{(T - F_s)}{(N - W)}\right\}$$

in which

T = measured horizontal feeder force (dynamometer D)

N = measured total vertical feeder load (summation of load cell forces A, B and C)

W = weight of the bulk solid entrapped in the interfacial zone

F_s = friction force on side skirts calculated using the expression in Appendix 2.

As the release angle β follows from simple geometry the apparent coefficient of internal friction, μ_{ia}, during steady-state operation can be calculated. No slip was allowed to occur at the belt surface. By measurement of the delivered volume over a period of time the velocity coefficient ξ at the aperture was determined. Because of the proven very good reproducibility, each test was repeated only once. The results for steady-state operation are shown in Table 1.

Table 1: Test results for steady-state operation

Material	Variation of aperture mm		μ_i	μ_{ia}	$\frac{\mu_{ia}}{\mu_i}$	ξ
	from	to				
Plastic granules	12	83	0.62 ± 0.030	0.470 ± 0.023	0.757 ± 0.028	0.863 ± 0.027
Spinach	20	100	0.74 ± 0.015	0.532 ± 0.017	0.719 ± 0.021	0.920 ± 0.068
Potato starch	19	90	0.55 ± 0.030	0.407 ± 0.02	0.740 ± 0.023	0.940 ± 0.072
Russian peas	28	53	0.56 ± 0.030	0.310 ± 0.011	0.554 ± 0.015	0.912 ± 0.040

It can be seen that the coefficient of "apparent" internal friction μ_{ia} is in the order of 0.7 to 0.8 times the coefficient of internal friction μ_i, with exception for the almost perfect spherical Russian peas. For those $\mu_{ia} \simeq 0.55\,\mu_i$.

The "break-away"-feeder drive force compared to the steady-state feeder drive force is given in Table 2.

Table 2: Results for "break-away" condition

Plastic granules	Spinach	Potato starch	Russian peas
1.59 ± 0.103	1.42 ± 0.04	1.46 ± 0.116	1.66 ± 0.143

5.1 Discussion of Results

For a large number of adjusted apertures films have been made of the flow along one of the side skirts, the bulk solid being provided with tracers. It was observed that both the local enclosed angles between the streamlines and the imaginary "planes of rupture" (one of which is indicated by EFGH in Fig. 4), and the velocity gradients did not change much when the aperture was varied. It is therefore clear that the apparent coefficient of friction μ_{ia} as defined earlier was approximately a constant fraction of μ_i for different apertures. As in all cases the ratio μ_{ia}/μ_i was smaller than unity, the required drive power for the feeder will not be underestimated when this ratio is taken as unity in the calculations. On the basis of the experimental results, however, 80 % of μ_i is a reasonable, and still safe, approximation for μ_{ia}.

6. Summary and Conclusions

1. The apron feeder is basically unsuited to an inclined (uphill) arrangement as this promotes loss of throughput, slip, wear and higher costs per ton of reclaimed bulk solid.
2. Ideal operation will only be achieved at the maximum allowable gate opening, depending on the kind of bulk solid, and with a continuously variable drive for the adjustment of the continuously required capacity.
3. Declined feeders require a smaller effective coefficient of friction at the belt, however this does not mean that the traction will also decrease; the contrary may be true within the range of considered inclination angles ($-20° \leqq \theta \leqq +20°$).
4. It is of extreme importance that the flow of bulk solid in the interfacial space between silo and feeder is continuously expanding during steady flow conditions.
5. Initial load has to be kept as low as possible which can be achieved by following the recommendation:
   a) It is recommended that the feeder is supported from the silo by elastic members that yield about 10 mm for a static head of about 4 times the load for steady flow conditions.
   b) Whenever possible, for instance when handling only one kind of bulk solid, the silo should not be emptied completely. A certain amount of material should be left instead, to a height of 3 to 4 times the effective width w of the feeder.

c) Whenever possible, filling operations of the silo should not be performed whilst the feeder is at a complete stop. Even running the feeder very slowly will reduce the initial load considerably.

6. The "apparent coefficient of friction" μ_{i_a} amounts to approximately 0.8 times μ_i.

7. Worked Example

The maximum required horsepower P during flow conditions has to be determined for an apron feeder running underneath a hopper for the handling of "Itabira" iron ore. Also the required traction T, effective coefficient of friction at the feeder belt μ_{be} and costs per reclaimed ton of ore should be estimated. The relevant data are given below.

Hopper

w = 1.5 m
l = 4.8 m
max. aperture a = 1.3 m
δ = 0.05 m
α = 24°

"Itabira" iron ore

ϕ_{if} = 45°
ϕ_w = 30°
ϱ = 2,850 kg/m³

Apron feeder

Max. motor speed 1,900 rpm
Sprocket wheel diameter = 1 m
Total mechanical speed reduction = 320
Horizontally arranged
Price per kWh = 16 Dutch cents

7.1 Solution

Either from Appendix 1 or the graphs shown in [19] it follows that H_{f_o} = 0.424. Taking $\phi_{i_a} \simeq \phi_{if}$ and $\mu_s \simeq \mu_w$ = tan $\phi_w \simeq$ 0.577 and assuming ϵ = 0.9, it follows, with l_o = 4.8/1.5 = 3.2, and δ_o = 0.05/1.5 = 0.033 and $a_{o_{max}}$ = 1.3/1.5 = 0.867 and $k = (1 - \sin \phi_{i_a})/(1 + \sin \phi_{i_a})$, and the appropriate formulae given before, including (21) and (23), that $T_o = P_o$ = 0.93.

The traction therefore amounts to $T = T_o \cdot w^3 \varrho g$ = 0.93 × 1.5³ × 9.81 × 2800 = 86,215 N. In particular from Equation (13) it follows that the effective coefficient at the feeder belt equals μ_{be} = 0.338. From the data provided it follows that the maximum feeder speed v_b equals 0.311 m/sec. So the required net feeder power equals:

$$P = P_o \cdot w^3 \varrho g \cdot v_b = T \cdot v_b = 86{,}215 \times 0.311 = 26{,}812 \text{ Nm/sec} = 26.81 \text{ kW}$$

The total efficiency of a reduction gear as large as 320, in series with an adjustable drive, will not be much better than 0.80. The real required power during flow therefore will be 26.81/0.8 ≃ 33.5 kW. The ideal throughput occurs when ξ = 1 and equals 1.5 × 1.3 × 0.311 × 9.81 × 3,600 = 5,990 × 10⁴ N/h ≃ 6,106 t/h. This corresponds with 33.5 × 16/6,106 = 0.088 Dutch cents per reclaimed ton of iron ore.

7.2 Discussion

By way of illustration the values of T_o, E_s and μ_{be} have also been calculated for smaller apertures and graphically displayed in Fig. 9.

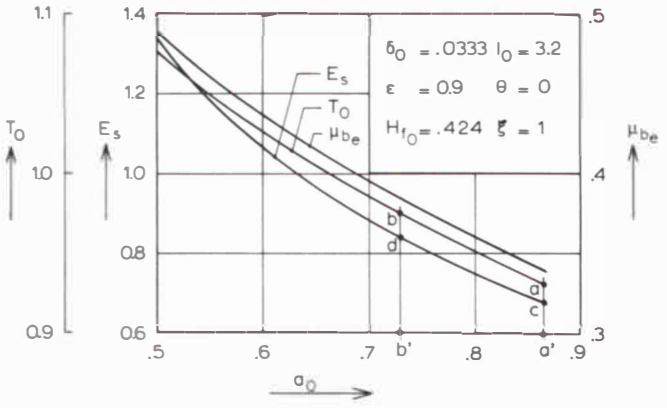

Fig. 9: Graphical representation for the worked example

If it is assumed that the speed of the electric motor can be reduced from 1,900 to 700 rpm in steps of 300, then a capacity slightly over (1,600/1,900) × 100 % of full throughput can only be achieved by throttling the valve from a_o = 0.867 to ≃ a_o = 0.73. According to the curves given in Fig. 9 this corresponds to a factor 1.05 in traction (points a and b) and a factor 0.842 in throughput or aperture (points a' and b'). Accounting for both effects means a factor of 1.05/0.842 ≃ 1.247 for the reclaim costs per ton of ore. This factor follows, of course, directly from comparing the E_s-values (points c and d). The reclaim price then amounts to 1.247 × 0.088 ≃ 0.11 cents per ton. As the capacity amounts to approximately (16/19) × 6,106 = 5,142 tons/h, this would mean on a 10 year basis of 1,800 h each: 10 × 1,800 × 5,142 × (0.11 — 0.088)/100 = 20,362 Dutch guilders. Although the feeder will not be in full time operation under these conditions, it still is worthwhile to consider the order of cost differences involved and to balance them, for instance, against the differences in capital costs for discontinuous and continuous variable speed drives and also their maintenance costs. Even if the unfortunate mode of operation discussed occurs for only 50 % of the time the inherent cost differences should still be considered because of a possible increase in wear at gate and feeder belt.

Controlling the throughput as described in this example means, according to the graph, that an effective coefficient of friction of 0.38 is required at the feeder belt. Assuming that the coefficient of friction at the belt equals that at the hopper wall, which is 0.577, the "safety factor" against slip amounts to 0.577/0.38 ≃ 1.52 leaving little opportunity for inclined arrangement and/or smaller valve openings.

Appendix 1

Feeder Load for Steady Flow Condition

The overpressure Q acting at the outlet of the converging section of a mass flow hopper during flow is given by:

$$Q = H_{f_o} \varrho g \cdot l w^2$$

in which H_{f_o} denotes the dimensionless overpressure factor, the analytical expression of which is given below:

$$H_{f_o} = \frac{1}{4 \tan \alpha} \left[\frac{Y}{X - 1} \left\{ \frac{1 + \sin \phi_{if} \cos 2\chi}{\sin \alpha} \right\} (\tan \alpha + \tan \phi_w) - 1 \right]$$

where

$$\chi = \frac{1}{2} \{ \phi_w + \arcsin (\sin \phi_w / \sin \phi_{if}) \}$$

$$X = \frac{\sin \phi_{if}}{1 - \sin \phi_{if}} \left\{ \frac{\sin (2\chi + \alpha)}{\sin \alpha} + 1 \right\}$$

and

$$Y = \frac{(\alpha + \chi) \sin \alpha + \sin \chi \cdot \sin (\alpha + \chi)}{(1 - \sin \phi_{if}) \sin^2 (\alpha + \chi)}$$

Appendix 2

Friction of Well Designed Side Skirts

The friction force per length dx on both side skirts, Fig. 4, amounts to:

$$F_s = 2 \cdot \sigma_{ah} \cdot h_x \cdot \mu_s \cdot dx$$

in which

- ϵ = coefficient taking account of the clearance between skirts and the feeder, Fig. 4, $0 < \epsilon < 1$
- σ_{ah} = average normal pressure on the side skirts
- μ_s = coefficient of kinetic friction at the interface of bulk and the side skirt
- h_x = local height of the side skirts below the schematized shear zone of the bulk material, Fig. 4.

If, on the basis of the release angle, a Rankine ratio between the horizontal and vertical pressures in the bed is presumed, it holds that $\sigma_{ah} \simeq k \cdot \sigma_{av}$. The symbol σ_{av} stands for the average vertical pressure which can be expressed in a static head H as already mentioned. The pressure profile over the skirt height, not being known, may decrease approximately linearly over the height and approach zero at the lower boundary of the skirt.

For practical reasons, however, a somewhat higher pressure can be expected. Therefore, a reasonable solution is to add half the local skirt height below the plane of shear in the bulk material to the head at the top of the bed H_f, so that:

$$\sigma_{ah} \simeq k \cdot \sigma_{av} \simeq k \cdot \left(H_f + \frac{h_x}{2 \cos \theta} \right) \varrho g$$

This corresponds with a total friction force on both side skirts per length element dx:

$$dF_{sx} \simeq 2k \left(H_f + \frac{h_x}{2 \cos \theta} \right) \varrho g \cdot h_x \cdot \mu_s \cdot dx$$

in which

$$h_x = \epsilon \frac{(a - \delta)}{l} \cdot x \qquad (0 < \epsilon < 1)$$

After integration over the slot length (l) arises:

$$F_s \simeq \frac{3}{2} k \mu_s \left(H_f + \frac{h_e}{2 \cos \theta} \right) \varrho g h_e l$$

in which h_e is the effective height being equal to:

$$h_e = \frac{2}{3} \epsilon (a - \delta)$$

Dividing by $\varrho g \omega^3$ results in the following dimensionless form:

$$F_{so} = \frac{3}{2} k \mu_s \left(H_{f_o} + \frac{h_{eo}}{2 \cos \theta} \right) h_{eo} l_o$$

in which

$$h_{eo} = \frac{h_e}{w} = \frac{2}{3} \epsilon (a_o - \delta_o)$$

Appendix 3

Friction of Badly Designed Skirts

In the case of the inferior outlet design, as illustrated in the lower left corner of Figs. 3 and 4, it can be assumed that the material that has been built up in the dead corners will stay there for a relatively long period of time. This makes it likely that the interfaces between this material and the side skirts will be free of shear stresses. Therefore σ_1 and σ_2 exerted on the dead corner material by the gate rim r and a length-friction l' of the side skirts, can be considered principal stresses so that the angle enclosed with the rim will be approximately:

$$\arctan (\pi/4 + \phi_{ia}/2).$$

Because the material flow converges between the dead corners, σ_2 can be expected to be greater than the vertical stress. However, the length l being of the same order as the aperture a, at the location of which the stress has almost completely dropped to zero, it is not very likely that such a passive stress field will fully develop. To illustrate the order of influence of the dead zones on the operation characteristics of the feeder, σ_2 will be taken equal to the vertical stress. The flow opposing force exerted by the dead corner material is equal to the forces exerted by the rims (r) on the dead material.

So it holds:

$$F'_s \simeq 2r \epsilon (a - \delta) \sigma_1$$

in which

$$\sigma_1 \simeq \frac{\sigma_2}{k} \simeq \frac{H_f \varrho g}{k}$$

and thus:

$$F'_s \simeq 2r\epsilon(a-\delta)\frac{H_f \varrho g}{k} = 2\frac{\epsilon}{k} r_o(a_o-\delta_o) H_{f_o} \cdot w^3 \varrho g$$

or in dimensionless form:

$$F'_{so} = 2\frac{\epsilon}{k} r_o(a_o-\delta_o) H_{f_o}$$

For the friction force F''_s along the remaining part of the side skirts, having a length of $l'' = l - l'$, similarly to the derivation in Appendix 2:

$$F''_s \simeq \frac{3}{2} k\mu_s \left(H_f + \frac{h''_e}{2\cos\theta}\right) \varrho g h''_e l''$$

in which

$$h''_e = \frac{2}{3}\left(1-\frac{l'}{l}\right)\epsilon(a-\delta);$$

$$l'' = l - l'$$

and

$$l' = r\tan\left(\frac{\pi}{4} + \frac{\phi_{ia}}{2}\right)$$

It also holds that:

$$F''_s = \frac{3}{2} k\mu_s \left(H_{f_o} + \frac{h''_{eo}}{2\cos\theta}\right) h''_{eo} \cdot l''_o \cdot w^3 \varrho g,$$

or in dimensionless form:

$$F''_{so} = \frac{3}{2} k\mu_s \left(H_{f_o} + \frac{h''_{eo}}{2\cos\theta}\right) h''_{eo} l''_o$$

in which

$$h''_{eo} = \frac{2}{3}\left(1-\frac{l'}{l}\right)\epsilon(a_o-\delta_o)$$

$$l''_o = \left(1-\frac{l'}{l}\right) l_o$$

and

$$\frac{l'}{l} = \frac{r_o}{l_o}\tan\left(\frac{\pi}{4} + \frac{\phi_{ia}}{2}\right), \qquad 0 < \frac{l'}{l} \leq 1$$

The total dimensionless friction force on the side skirts in case of this inferior design F_{swo} follows from:

$$F_{swo} = F'_{so} + F''_{so}$$

Appendix 4

Measures to Increase the Apparent Coefficient of Friction at the Feeder Plates

When the feeder plates are provided with dams or ribs perpendicular to the direction of feeder travel, a considerable increase in apparent friction coefficient is achievable. The reason is that a continuously changing small amount of bulk acts as if it were made a constructional member of the feeder plates, as illustrated in Fig. 10, i.e., when enough

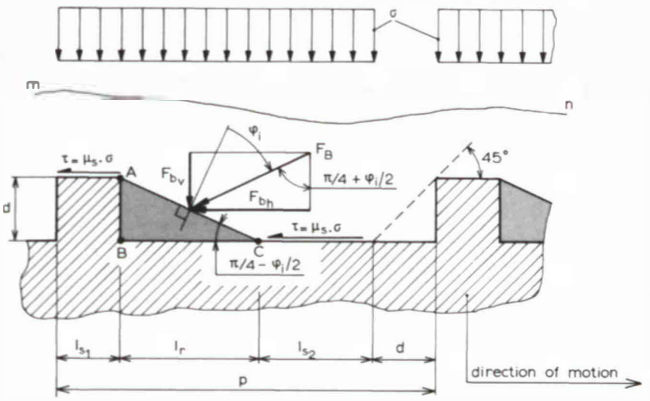

Fig. 10: Plate surface geometry in case of dams of square cross-section

particles much smaller than the dam height are available to fill up prismatic spaces, the cross-section of which are indicated by ABC in the illustration. Because of the internal friction of the bulk, the pressure on the plates in the zone just behind the dams will be very low. For the purpose of estimation this pressure is presumed to be zero over a length equal to the dam height. When, furthermore, the coefficient of friction between the bulk and (steel) feeder plates is denoted by μ_s and the internal steady flow bulk friction coefficient by ϕ_i, the following equations representing the total friction and normal forces per pitch length p and unit width are easily derived from the geometry of the illustration:

$$\Sigma F = \left(l_{s_1} + l_{s_2}\right)\mu_s\sigma + F_{bh}$$

in which the first term stands for the friction force at the steel interface and F_{bh} for the horizontal component of the inter-bulk force F_b exerted on the "dead corner" material ABC, collected just ahead of a dam:

$$\Sigma N = (p-d)\sigma$$

The apparent, or equivalent, coefficient of friction at the belt interface amounts to:

$$\mu_{bd} = \frac{\Sigma F}{\Sigma N} = \frac{\left(l_{s_1} + l_{s_2}\right)\mu_s\sigma + F_{bh}}{(p-d)\sigma}$$

When $l_{s_1} + l_{s_2} = p - d - l_r$ and $F_{bh} = F_{bv}\tan(\pi/4 + \phi_i/2) = \sigma \cdot l_r \cdot \tan(\pi/4 + \phi_i/2)$

the following holds:

$$\mu_{bd} = \frac{(p-d)\mu_s + l_r\{\tan(\pi/4 + \phi_i/2) - \mu_s\}}{(p-d)}$$

where $l_r = d/\tan(\pi/4 - \phi_i/2)$.

This expression can be transformed into:

$$\mu_{bd} = \mu_s + \frac{d/p}{1-d/p}\left\{1 + (\mu_i + \sqrt{1+\mu_i^2})(2\mu_i - \mu_s)\right\}$$

When $l_{s_1} = d_1$ this formula holds on condition that:

$$\frac{d}{p} \leqq \frac{1}{2 + \mu_i + \sqrt{1 + \mu_i^2}}$$

Fig. 11 shows some results. Point P illustrates by way of example that, in case $\mu_s = 0.35$ and $\mu_i = 0.8$ and $p/d = 0.1$, the apparent coefficient of friction equals $\simeq$ 0.74, i.e., approximately twice the original value of 0.35.

The solid horizontal lines indicate the condition from where a further increase of d/p leads to $\mu_{bd} > \mu_{if}$, indicating that a slip zone might arise somewhere inside the bulk material as illustrated by the line m — n in Fig. 11.

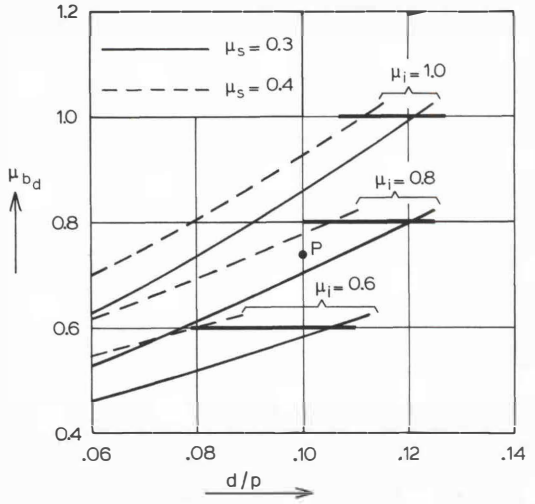

Fig. 11: Illustration of the extent to which the kinetic coefficient of friction at the interface of the bulk material and flat steel pans can be increased by providing the pans with dams

The small extra amount of material that will drop from the idling (returning) feeder part will certainly not cause any problems in cases where a spill conveyor has been provided for.

Acknowledgements

The author wishes to thank Mr. H. J. Rietman for writing the computer program, and Mr. J. Bosboom and Mr. M. Valkman for technical assistance.

References

[1] Jonkers, C. O., "The loss factor of transport", Fördern und Heben, Vol. 31 (1981), February, pp. 98—102

[2] Arnold, P. C., McLean, A. G. and Roberts, A. W., "Bulk Solids: Storage, Flow and Handling", TUNRA-Bulk Solids Handling Research Associates (1980)

[3] Shannon, G. A., "Silo feeders and discharge drives with their related controls", IEEE Trans. Ind. Appl., Vol. 1A-15 (1979), No. 4, pp. 348—356

[4] Block, S., "Plattenbänder als Bunkeraustrags- und Aufgabeförderer", Aufbereitungs-Techn., (1978) No. 11, pp. 555—558

[5] Rademacher, F. J. C., "Gestaltung von Bunkerausläufen für den Austrag mit Abzugsbändern", Aufbereitungs-Tech., (1978), No. 9, pp. 422—427

[6] Zosel, F., "Abzugsvorrichtungen für grobkörnige Schüttgüter", Aufbereitungs-Techn., (1978), No. 8, pp. 350—353

[7] Johanson, J. R., "Storage and flow of solids", 3 Day Working Seminar Notes, Australian Mineral Foundation, Adelaide, July 1976

[8] Bruff, W., "Industrisiloer", Ingeniorforlaget A/S, 1974 (in Norwegian)

[9] Winkler, W. A., "The Bougainville 975 TPH feeder", Trans. ASME, J. Eng. Ind., (1973), February, pp. 27—30

[10] Doeksen, G., "Precautions in order to attain design capabilities of mass flow systems", Transac. ASME, Journal of Eng. Ind., (1973), February, pp. 93—96

[11] Larson, P., "Improving the flow of lead-zinc ore", ASME paper 72-MH-23

[12] Reisner, W. and Eisenhart Rothe, M. von, "Bins and Bunkers for Handling Bulk Materials", Trans Tech Publications, 1971

[13] Colijn, H. and Hanson, P. D., "Practical applications of hopper and bin design", Can. Min. Met. (1970)

[14] Johanson, J. R., "Feeding", Chem. Eng. Deskbook Issue, (1969), Oct. 13, pp. 75—83

[15] Colijn, H. and Carrol, P. J., "Design criteria for bin feeders", Soc. Min. Eng. Trans. AIME, Vol. 241 (1968), pp. 389—404

[16] Allen, D. S., "Bulk material flow through hoppers and feeders", Chem. Eng. Pr., Vol. 62 (1966), p. 65

[17] Hager, M., "Untersuchungen zur Befüllung und zum Gutaustrag von Bunkern mit Abzugsbändern", Stahl und Eisen, Vol. 86 (1966), No. 8, pp. 457—465

[18] Hager, M., "Untersuchungen zur Befüllung und zum Gutaustrag von Bunkern mit Abzugsbändern", Dissertation, University of Hannover, Germany, (1965)

[19] Jenike, A. W., "Storage and Flow of Solids", Bulletin No. 123, University of Utah, (1964)